Electronic Activation of a DNA Nanodevice Using a Multilayer Nanofilm

Hyejoong Jeong, Simona Ranallo, Marianna Rossetti, Jiwoong Heo, Jooseok Shin, Kwangyong Park, Francesco Ricci, and Jinkee Hong**

***A** method to control activation of a DNA nanodevice by supplying a complementary DNA (cDNA) strand from an electro-responsive nanoplatform is reported. To develop functional nanoplatform, hexalayer nanofilm is precisely designed by layer-by-layer assembly technique based on electrostatic interaction with four kinds of materials: Hydrolyzed poly(β-amino ester) can help cDNA release from the film. A cDNA is used as a key building block to activate DNA nanodevice. Reduced graphene oxides (rGOs) and the conductive polymer provide conductivity. In particular, rGOs efficiently incorporate a cDNA in the film via several interactions and act as a barrier. Depending on the types of applied electronic stimuli (reductive and oxidative potentials), a cDNA released from the electrode can quantitatively control the activation of DNA nanodevice. From this report, a new system is successfully demonstrated to precisely control DNA release on demand. By applying more advanced form of DNA-based nanodevices into multilayer system, the electro-responsive nanoplatform will expand the availability of DNA nanotechnology allowing its improved application in areas such as diagnosis, biosensing, bioimaging, and drug delivery.*

1. Introduction

DNA has become one of the most important biological materials: its ability to self-assemble in a highly predictable manner, its low synthesis cost and biocompatibility have been utilized to develop a variety of nanostructures and functional DNA-based nanodevices for biomedical applications.[1–3] For example, sequences of DNA are rationally designed to recognize a specific target molecule and convert the recognition event into a useful function (i.e., signal production or release of a cargo).[4–12] Despite the great advantages represented by such nanodevices, their target-induced actuation is usually achieved by exogenously adding them into a sample.[13] To make a better control of activating DNA-based nanodevices, we need to find a precisely controllable way out of common basic mechanism.

In response to this, finding new strategies to modulate the activation of DNA-based nanodevices would be crucial to their development for nanotechnology applications. Here we report the use of a multilayer nanofilm that is used to release a DNA strand in a controlled fashion using electrochemical inputs. More specifically, we prepared a multilayer nanofilm on the surface of a chip-electrode using a layer-by-layer (LbL) assembly method.[14] Using this method, multilayers can be fabricated by alternating adsorption of a charged substrate from an aqueous solution. Conventionally, polymers are used in this approach, and recently a broad

H. Jeong, J. Heo, Prof. J. Hong
Laboratory of Functional Nano Films
School of Chemical Engineering and Material Science
Chung-Ang University
Seoul 06974, Republic of Korea
E-mail: jkhong@cau.ac.kr

S. Ranallo, M. Rossetti, Prof. F. Ricci
Chemistry Department
University of Rome Tor Vergata
Via della Ricerca Scientifica
Rome 00133, Italy
E-mail: francesco.ricci@uniroma2.it

J. Shin, Prof. K. Park
Laboratory of Organic Materials
School of Chemical Engineering and Material Science
Chung-Ang University
Seoul 06974, Republic of Korea

DOI: 10.1002/smll.201601273

range of charged molecules are used such as proteins, growth factors, small molecules, drugs, particles, and DNA, which may be adsorbed while retaining their forms and activities.[15–20] In recent years, stimuli-responsive LbL-assembled films that are controlled by external stimuli, such as pH, water, electricity, and temperature, have been reported.[21–24] LbL multilayer films are versatile and may be prepared with controllable thicknesses at the nanoscale. Consequently, functional LbL films are being developed as a platform for future nanodevices.

In this approach, we incorporated a complementary DNA (cDNA) strand activating DNA devices into the multilayer film. Taking advantage of the drop LbL assembly method, we coated multilayer films with a small amount of cDNA onto various substrates, including a silicon wafer and a chip-electrode (**Figure 1**A). We fabricated the electro-responsive multilayer film as follows: $(PBAE/DNA/rGO+/DNA/rGO+/PEDOT:PSS)_{n1}$–$(rGO+/rGO–)_{n2}$, where PBAE indicates poly(*β*-amino ester); DNA is a cDNA; rGO indicates reduced graphene oxide; PEDOT:PSS is poly(3,4-ethylenedioxythiophene)-poly(styrene sulfonate), and then *n*1 and *n*2 indicate number of hexalayer and bilayer, respectively. Each material was sequentially adsorbed onto a silicon wafer or a chip-electrode *n* times based on electrostatic interaction. The structure of hexalayer can be rationalized as follows: first, the positively charged PBAE can release DNA due to its hydrolytically degradable property.[25] Secondly, the negatively charged DNA may be efficiently entrapped by the positively charged rGO layers, mainly due to electrostatic interaction, partially additional hydrophobic and *π*-stacking interactions.[26–28] By repeating this deposition, we can incorporate DNA proportionally to the thickness of the film. Thirdly, the negatively charged PEDOT:PSS helps to increase the conductivity of the film for the purpose of controlling DNA release more efficiently. To avoid spontaneous release of DNA, rGO bilayers were deposited on the outermost hexalayer film by electrostatic interaction between oppositely charged rGOs. According to the previous report in our group, graphene oxide (GO) layer acted as a barrier to prevent spontaneous protein release.[29] Using this multilayer film, we developed DNA nanodevice activating system by electronic inputs.

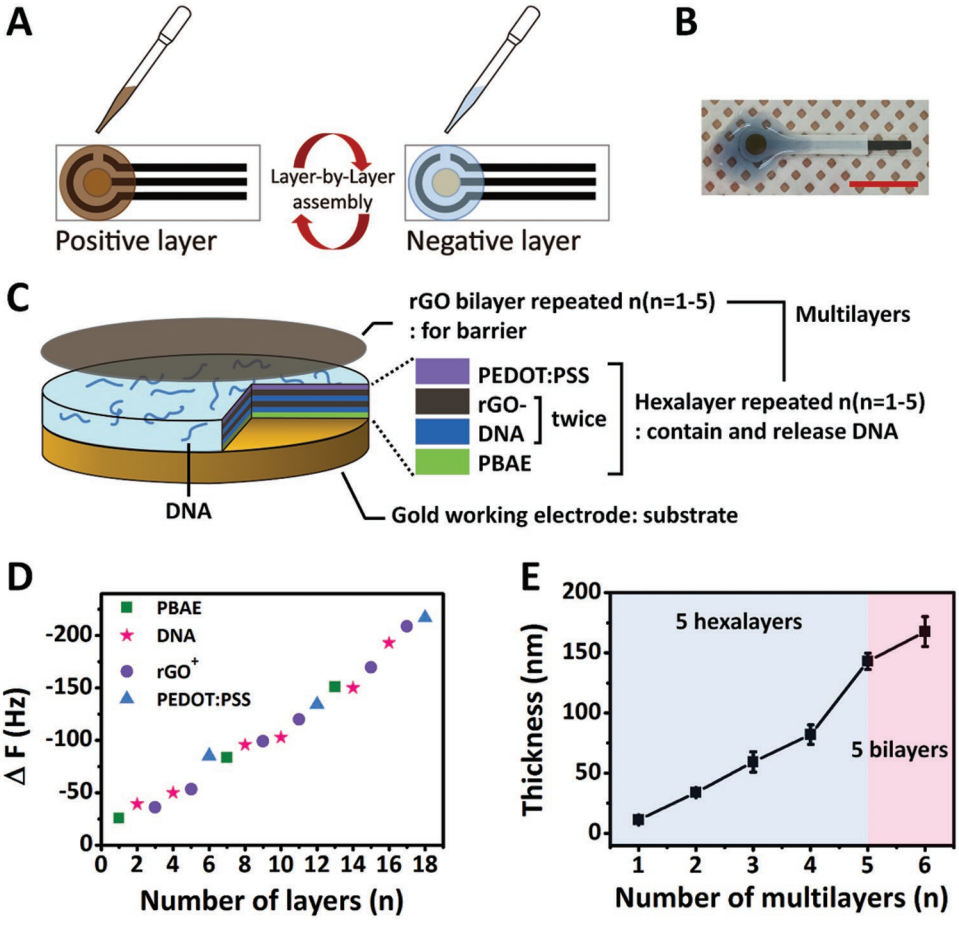

Figure 1. A) A schematic representation of the drop LbL process for producing multilayer films on a chip-electrode. B) A photographic image of only working electrode of a chip-electrode in the process of LbL, specifically PEDOT:PSS layer deposition. Scale bar indicates 1 cm. C) A schematic illustration of multilayer film composed of $(PBAE/DNA/rGO+/DNA/rGO+/PEDOT:PSS)_{n,\,(n=1-5)}$ hexalayers and $(rGO+/rGO–)_{n,\,(n=1-5)}$ bilayers on an electrode. Deposition of multilayer film determined by QCM and profilometer: D) Frequency shifts of each layer up to three hexalayers. E) Thickness growth curve of multilayers composed to hexalayers from number 1 to 5 and $(rGO+/rGO–)_5$ bilayers at number 6.

DOI: 10.1002/smll.201601273

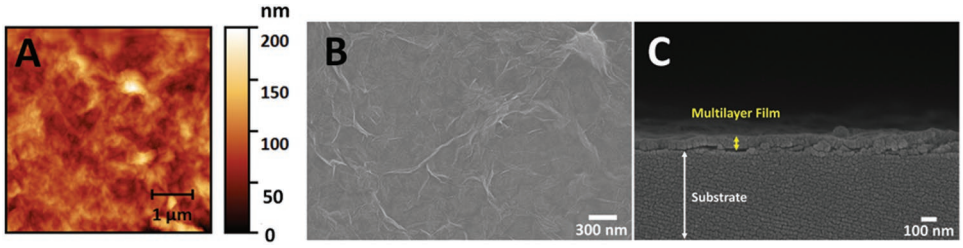

Figure 2. Film morphologies characterized by AFM and SEM. A) AFM topographic image of the outermost rGO barrier layer. SEM micrographs of equal film B) observed from the top and C) in cross-section.

2. Results and Discussion

2.1. Multilayer Film Characterization

2.1.1. Fabrication of DNA Contained Multilayer Film Based on Drop LbL

We used the drop LbL assembly method to coat a chip-electrode with DNA (Figure 1A). The drop LbL method was first reported by Watanabe et al. in 2009.[30] They determined that dip-coating and drop-coating of films resulted in similar frequency shifts with each layer addition in a quartz crystal microbalance (QCM) analysis. Thus, there is no significant difference between films using the two processes. Furthermore, the drop LbL method has several advantages over the conventional dipping method. Multilayer nanofilms can be fabricated using a smaller amount of solution than dipping (50 μL per layer). The drop LbL method can produce a multilayer film confined to a particular area of a substrate. The insulating ink onto chip-electrodes is prone to separation from the polyester film due to the large amount of water in the dipping method. For these reasons, we used the drop LbL assembly method outlined by previous research.[30]

To evaluate the layer deposition by the drop LbL assembly method, QCM determined the frequency decrease which is proportional to the mass increase (Figure 1D). The linear frequency decrease indicates that the hexalayers are deposited successfully. To compare deposition of each material, the average frequency shift and mass alteration per hexalayer can be calculated as follows: PBAE (–13.6 Hz, corresponding to 0.2 μg cm^{-2}), DNA (–22.2 Hz, 0.4 μg cm^{-2}), rGO+ (–18.6 Hz, 0.3 μg cm^{-2}), and PEDOT:PSS (–17.9 Hz, 0.3 μg cm^{-2}). The mass increase of materials is in the order of DNA > rGO+ > PEDOT:PSS > PBAE. From this result, we determined that the hexalayer film has a high affinity for DNA incorporation. Furthermore, we can estimate the approximate amount of DNA deposited on the working electrode of a chip-electrode (area, 7.5 mm^2).

To ensure that the multilayer film was produced uniformly, a thickness growth curve was plotted. The thickness of the film increases uniformly with each hexalayer an average of 23.6 nm until four hexalayers (Figure 1E). With the addition of the fifth hexalayer, the thickness increases by 61.0 nm, approximately three times higher than the previous average increase. This is because rGO aggregation was intensified due to the largest surface area at fourth hexalayers. In the graph, the error bars showed that little undulation on the surface continuously increased corresponding to the layer increase by rGO aggregation. RGO is a fragile material easily aggregated at certain pH values or by ionic strengths due to reduced functional groups. In the film, rGO was introduced between the DNA and the PEDOT:PSS layers, and could be aggregated by contacting with the DNA buffer (50×10^{-3} M of sodium phosphate and 150×10^{-3} M of sodium chloride, pH 7.0) and the PEDOT:PSS solution (pH 2.8). The sixth layer consisted of rGO which is a form of 2D sheet. The entire 10 layers have a thickness of only 24.7 nm. In fact, each sheet has a thickness of 1 nm, but in this case the thickness measurement is higher than our estimation due to the high surface variation, as indicated by the larger error bar.

2.1.2. Characterization of Multilayer Film Morphology

The 2D-topographic image obtained by atomic force microscopy (AFM) provides roughness information (**Figure 2**A). The root-mean-square (RMS) indicates a relatively high roughness value of 18.9 nm. As reported previously, five bilayers of GO deposited onto a relatively rough surface (RMS = 3.7 nm) resulted in a very smooth surface (RMS < 1).[29] GO can coat a rough surface more uniformly. With reference to this report, we assume that our five hexalayer film (i.e., without the barrier layer) has a higher roughness, and the rGO-based barrier layer coated the surface more uniformly and without undulation. Furthermore, we can identify the form of the surface graphene sheets by AFM topography.

We further analyzed the films by scanning electron microscopy (SEM) (Figure 2B). As with the AFM topography, the rGO sheets are observed in a magnified form. The cross-section of the film confirms that our film has a highly uniform structure (Figure 2C).

2.2. Activating Mechanism of a DNA Nanodevice

We validated our strategy using a basic linear DNA nanodevice labeled at the two ends with a fluorophore/quencher optical pair. Before activation, the linear DNA nanodevice is in a random coil conformation form and thus in an "OFF" state. In the presence of a complementary DNA strand (cDNA), the nanodevice undergoes a conformational change to a rigid duplex conformation, and the switch is "ON"

DOI: 10.1002/smll.201601273

www.MaterialsViews.com

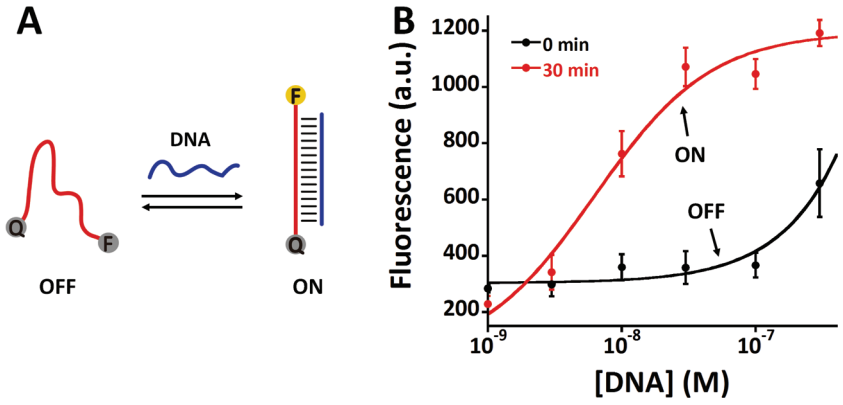

Figure 3. A) A schematic diagram of a DNA nanodevice activated by a cDNA strand. The "OFF" state of DNA nanodevice changes to the switched "ON", resulting in fluorescence (F: fluorophore, Q: quencher). B) Binding curves for the DNA nanodevice exposed to a cDNA strand. The lower fluorescence at 0 min indicates an OFF state (black line). The higher fluorescence after 30 min indicates an ON state (red line) through saturated activation of the DNA nanodevice.

leading to an increase in fluorescence signal. This simple concept is illustrated in **Figure 3**A.

To quantify the performance of the DNA nanodevice, a binding curve is required as a standard calibration curve (Figure 3B). We used the Langmuir model, which is the most basic binding model reported by O'Shannessy et al. in 1993.[31,32] From this model, the equilibrium dissociation constant (K_D) was obtained and used for calculating concentration of cDNA strands. The details of equation and calculation process of K_D are described in the Supporting information.

In Figure 3B, only the two curves of OFF state (at 0 min) and ON state (at 30 min) are shown. All the other curves, measured every 5 min up to 45 min, are provided in the Figure S1 in the Supporting Information. The successfully obtained binding curve was used to calculate the molar concentration of the nanodevice activated by cDNA.

2.3. Control of DNA Nanodevice Activation via Electrostimuli

2.3.1. Applied Different Electrostimuli to Activate a DNA Nanodevice

As shown in **Figure 4**A, we applied two kinds of electrical potentials to the chip-electrode coated with the DNA containing multilayer nanofilm. As a control, another chip-electrode was dipped into a DNA buffer to determine the spontaneous release of DNA by diffusion. In this process, DNA nanodevice was activated by cDNA strand released from the electrodes, leading to fluorescence. Based on the fluorescence intensity, we acquired the molar concentration of activated DNA nanodevice using binding curves in Figure 3B. According to the Langmuir equation, the DNA nanodevice binds with cDNA in a 1:1 ratio. For this reason, the concentration of activated DNA nanodevice is equal with the molar concentration of cDNA released from the multilayer film onto a chip-electrode.

We applied both oxidative (positive) and reductive (negative) potentials, as indicated by the black and red points in Figure 4B. Each point represents different potentials (from 0.0 to 0.7 V or from –0.7 to 0.0 V, at intervals of 0.1 V) applied for 30 s in a chronological sequence. The offering periods of factors are indicated by the translucent bars attached to the individual points. In the process, the current is increased as a function of the applied potential, as shown in the Supporting information (in particular, the insets of Figure S2). In comparison between black and red graphs, we determined that the DNA nanodevice is activated more by applying reductive potential than oxidative potential. We concluded that reductive potential could completely reduce the functional groups in rGO, and eliminate charges as well.[33] As shown

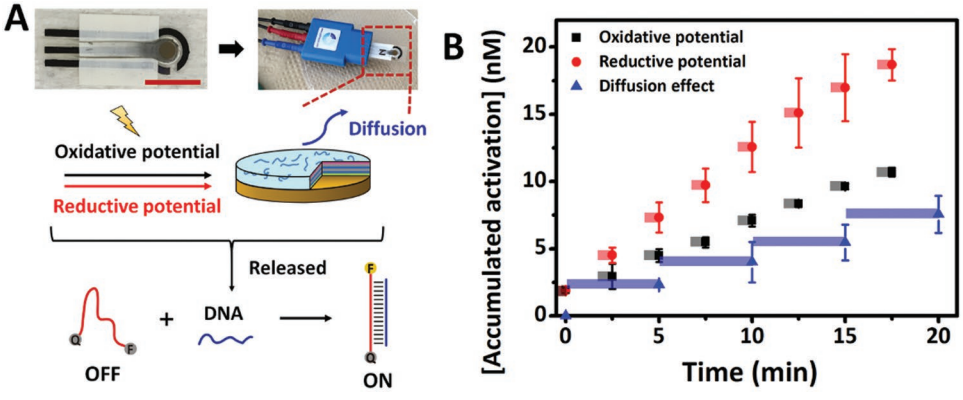

Figure 4. A) Photographic images indicate chip electrode fabricated a multilayer film (left) and connected to potentiostat. Scale bar is 1 cm. The multilayer film on a working electrode in the red box as dotted line is magnified to an illustration under photographs. A schematic image of activation process of the DNA nanodevice binding with cDNA released via three factors, including oxidative potential (black), reductive potential (red), and the diffusion effect (blue). B) Accumulated concentration of DNA nanodevice activated by oxidative potentials from 0.0 to 0.7 V (■, black squares), reductive potentials from –0.7 to 0.0 V (●, red circles), and diffusion for 20 min (▲, blue triangles). The translucent bars that are attached each point indicate the offering period of factors. The black and red bar indicate 30 s and the blue bar indicates 5 min.

small 2016,
DOI: 10.1002/smll.201601273

Table 1. Comparison of quantitative DNA release by the three different factors.

Contained DNA in a film onto a chip-electrode [ng]		Activated DNA nanodevice [nM]	Released DNA [ng]	Release ratio [%]	Release ratio for 4 min [%]
147.7	Oxidative	10.7	6.3[a)]	4.2	
	Reductive	18.7	10.9[a)]	7.4	
	Control	7.6	4.4[a)]	3.0	0.6

[a)]Calculated using M_w of cDNA (5847) and 100 uL of volume.

in Figure S2B in the Supporting Information, electrons can transfer readily to the fully reduced GO multilayer, allowing the DNA to be quickly released. In comparison, the DNA is less readily released by oxidative potential due to the insufficient reduction of rGO.

To compare the effect of the electronic stimuli to a control, a coated chip-electrode was dipped into the buffer for a period of 20 min. Spontaneous release of DNA, shown by the blue points in Figure 4B, was not completely prevented, but was found to be much lower than with the electronic stimuli. Because hydrolysis of PBAE occurs rapidly (the half-life is 7–8 h at pH 5.1).[25] The DNA can be released through cracks between the layers following a decrease in electrostatic interactions with the PBAE. However, considering the total release time, the amount of DNA diffused from the electrode is not significant.

2.3.2. The Multilayer Nanofilm as a Platform for Controlling DNA Nanodevice

The overall results are summarized in **Table 1**. The quantity of DNA in the five hexalayers deposited onto the chip-electrode was calculated using the QCM results in Figure 1D. DNA of ≈147.7 ng can be deposited onto each chip-electrode, considering the only area of working electrode (7.5 mm^2). The amount of released DNA (ng) was calculated using the molecular weight of cDNA and 100 uL of volume. In comparison with the total quantity of deposited DNA in the five hexalayers, cDNA is released at 4.2%, 7.4%, and 3.0% by oxidative stimuli, reductive stimuli, and diffusion, respectively. The total release time with electronic stimuli is 4 min, while that of the control is 20 min. Therefore, when we take an equal releasing time of 4 min into consideration, the DNA released from the control is negligible (only 0.60%). Conversely, much more DNA was released by electronic stimuli, in particular by reductive inputs. Since over 90% of the DNA was still contained in the multilayer film, we estimate that multilayer coated chip-electrode would be continually used for activating DNA nanodevice. From this result, we controlled activation of DNA nanodevice using two kinds of electronic stimuli via multilayer film and quantitatively calculated concentration of DNA nanodevices at nanoscale.

3. Conclusion

In this study, in response to the needs of DNA nanotechnology development, we demonstrated a method to regulate the spontaneous activation of DNA nanodevice by introducing on demand cDNA release system of an electroresponsive multilayer nanofilm. Through the drop LbL assembly method, we successfully fabricated multilayer nanofilms onto a gold-based chip-electrode efficiently including DNA. The nanofilms incorporated and released DNA by applying small electronic inputs, and showed quick response to reductive potentials. Eventually, the released DNA could quantitatively activate a DNA nanodevice. To the best of our knowledge, this is the first attempt to adjust DNA nanodevice using multilayer nanofilm. On the basis of our report dealing with the most basic form of DNA nanodevice, we can modulate it into more advanced forms using other kinds of triggers or functional DNA-based nanodevices including various functions such as drug delivery, pH-responsibility, and enzyme or gene detection for biomedical applications. We believe our approach can provide a new platform to DNA-based nanodevices. For future follow up studies, we will control activation of functionalized DNA nanodevices performing more specific biomedical assignments.

4. Experimental Section

Materials: Graphite (20 micron) was obtained by Alfa aesar (Ward Hill, MA, USA). PBAE was synthesized as previously described.[25] rGO were synthesized from 20 μm of graphite according to previous report.[34] PEDOT:PSS PH-1000 M122 was purchased from Ossila Ltd. (Sheffield, UK). Complementary sequence of DNA (Sequence: 5′- CAGAGACTGGTCAGCACAG-3′, M_w 5847) was purchased from Aldrich (St. Louis, MO).

Synthesis of Poly (β-Amino Ester): Poly (β-amino ester) was synthesized in accordance with the method of polymer 2 in previous research.[25] Therefore, a brief synthetic process was described. The reaction was carried out under an inert atmosphere of N_2. Piperazine and 1,4-butanediol diacrylate were purchased from Aldrich (St. Louis, MO). Tetrahydrofuran (THF) was distilled from sodium-benzophenone ketyl just prior to use. ^{1}H-NMR (600 MHz) and ^{13}C-NMR (150 MHz) were acquired using $CDCl_3$ as a solvent and tetramethylsilane (TMS) as an internal standard. Chemical shifts are reported in δ units (ppm) by assigning the TMS resonance in the ^{1}H-NMR spectrum as 0 ppm and the $CDCl_3$ resonance in the ^{13}C-NMR spectrum as 77.2 ppm. All coupling constants, *J*, are reported in hertz (Hz). Gel permeation chromatography (GPC) (Ultimate 3000, Thermo) analysis was performed using THF.

Procedure for Preparation of Poly (β-Amino Ester): To the solution of 1,4-butanediol diacrylate (1.00 mL, 5.30 mmol) in THF (5.00 mL) was added to the solution of the piperazine in THF (5.00 mL). The reaction mixture was heated at 50 °C and stirred for 50 h. The reaction mixture was cooled to room temperature and poured slowly into vigorously stirring hexane (100 mL). The precipitated powder was recovered by filtration and dried under vacuum to yield the desired poly(β-amino ester) (1.025 g, 68.0%) as a white powder: IR (KBr): ν = 2948 (s), 2818 (s), 1731 (s), 1463 (m), 1188 (s),

1156 (s); ^{1}H-NMR (600 MHz, $CDCl_3$, δ) 4.10 (br t, 4H), 2.67 (t, J = 7.41 Hz, 4H), 2.49 (t, J = 7.41 Hz, 4H), 2.43–2.52 (br m, 8H), 1.67–1.72 (br m, 4H); ^{13}C-NMR (150 MHz, $CDCl_3$, δ) 172.39 (2C), 63.87 (2C), 53.49 (2C), 52.82 (4C), 32.27 (2C), 25.25 (2C).

GPC (THF, polystyrene (PS) standard): M_n = 2410; M_w = 5706; polydispersity index (M_w/M_n) = 2.37.

Synthesis of Graphene Oxide: GO was produced by a modified Hummer's method from graphite powder (20 um, Alfa aesar). To obtain negatively charged GO (GO-COO^-), carboxylic acid groups were introduced using oxidation through acid treatment. Concretely, graphite powder (1 g) was treated with H_2SO_4 (4 mL), $K_2S_2O_8$ (0.8g), and P_2O_5 (0.8 g) at 80 °C. After stirring the mixture for 4.5 h, it was washed using ≈1.3 L distilled water which was slowly added to the mixture and removed by filtration. The remaining slurry was dried overnight in ambient condition. The peroxidized powder was dissolved in concentrated 26 mL of H_2SO_4 at 0 °C. Then $KMnO_4$ was slowly added to solution cooling in the cold water bath to keep the temperature below 30 °C. After stirring for 2 h at 36 °C, 46 mL of distilled water was slowly added to the solution maintaining the temperature below 60 °C after stirring for 2 h at 26 °C. To terminate the reaction, 140 mL of distilled water and 2.5 mL of 30% H_2O_2 solution were added in the mixture. This solution was filtered with 350 mL 10% HCl solution for washing. Lastly, prepared solution was dialyzed to eliminate the residual acidic ions.

GO-COO^- powder was dissolved in pH 4.3 distilled water at 0.05% (w/w) and dispersed using ultrasonication. To prepare positively charged graphene oxide (GO-$NH3^+$), carboxyl groups of negatively charged GO-COO^- was functionalized with amine groups by EDC mediated reaction using excess ethylenediamine. Dialysis was needed to remove excessive reactants and by products for 1 week. The pH of GO-COO^- and GO-$NH3^+$ solutions was used as intact values.

Synthesis of Reduced Graphene Oxides: Each of the prepared negatively charged GO-COO^- and positively charged GO-$NH3^+$ (0.05% (w/w), 20 mL, respectively) was reduced with 24 µL of hydrazine (N_2H_4, Aldrich) and 112 µL of 30% ammonia solution (NH_3, Junsei, Japan). Each mixture solution was stirred for 10 min and put in 90 °C oven for 2 h closing a cap loosely. The final solution was dialyzed to remove residual.

Preparation of Solutions for LbL: PBAE was dissolved in pH 5.2, 100×10^{-3} M sodium acetate buffer (NaOAc) at 1 mg mL^{-1} (Aldrich) and final pH is 4.8. The rGO solutions were fixed to 0.05% (w/w) without any ionic salts. The pH conditions unadjusted of each rGO-COO^- and rGO-NH_3^+ were 9.7 and 8.0, respectively. 1% (w/w) of PEDOT:PSS solution was diluted 10 times with distilled water to 0.1% (w/w) and the final pH value was 2.8. The buffer for DNA was prepared by mixture of 50×10^{-3} M of sodium phosphate (Na_3PO_4) and 150×10^{-3} M of sodium chloride (NaCl) adjusted pH value to 7.0 using 1 M HCl (designated "DNA buffer"). The cDNA solution was prepared at 10×10^{-6} M in the buffer. The washing solutions of PBAE and both rGOs were prepared to equal pH conditions with above solutions in distilled water.

Drop LbL Film Construction: The composition of multilayer film was $(PBAE/DNA/rGO^+/DNA/rGO^+/PEDOT:PSS)_{n1}-(rGO^+/rGO^-)_{n2}$, ($n$ = number of layers). The film consisted of two parts: the first part included DNA and the second part was composed of rGOs as a barrier layer. The substrate was gold-based chip-electrode prepared as previous report.[35] In brief, the chip-electrode was produced by a screen printing machine (245 DEK, Weymouth, UK). Three kinds of conductive inks including graphite, gold, silver-based, and one insulating ink were printed on a polyester film (Autostat HT5). The final chip-electrode constituted of gold-based working electrode, carbon-based counter electrode, and platinum-based reference electrode. The area of working electrode was 0.07 cm^2 (diameter was 0.3 cm). To construct multilayer film on the surface of a chip-electrode and a cleaned wafer were modified to negative charges using oxygen plasma (CUTE-1B, Femto science). A 50 µL drop of PBAE solution was put on the negatively charged electrode for 10 min and followed by two washing steps to dip the electrode into pH-adjusted (4.8) distilled water for 1 min each. Then equal volume of DNA solution was put on the electrode for 10 min and implemented same washing steps with DNA buffer. In the equal way above, positively charged rGO+ was deposited on the electrode and washed with pH-adjusted (8.0) distilled water. Then DNA and rGO+ were deposited again. The last layer is PEDOT:PSS and washed with intact distilled water. $(PBAE/DNA/rGO+/DNA/rGO+/PEDOT:PSS)_n$ multilayer film could be fabricated by repeating the process n times. For the barrier layer, rGO multilayer was produced on the DNA incorporating film. rGO+ and rGO− layers were produced with washing steps using pH-adjusted (8.0 and 9.7, respectively) distilled water. $(rGO+/rGO-)_n$ barrier film was fabricated by repeating this process n times. Drying step was not required to keep moisture for DNA stability.

Film Characterization: The multilayer film was characterized on the silicon wafer due to the lack of uniformity of chip-electrode. The thickness of multilayer films was obtained from profilometer (Dektak 150, Veeco) and the quantitative analysis of each layer was implemented using a QCM (QCM 200, 5 MHz, SRS). 2D topographic image was obtained from an AFM(NX-10, Park systems). The top and cross-section micrographs of multilayer film were acquired from a field emission scanning electron microscopy (SIGMA, Carl Zeiss).

Detection of DNA Nanodevice Activation and Quantitative Analysis: The sequence of used DNA nanodevice was labeled with FAM (5-carboxyfluorescein) and OQA (Onyx Quencher) (Sequence: 5′-(FAM) ACTCA CTGTGCTGACCAGTCTCTG ACTCG (OQA)-3′, M_w 9861) and complementary DNA sequence mentioned in "Materials" section were purchased from Aldrich. The stock of both DNAs were dissolved in the 50×10^{-3} M sodium phosphate buffer adjusted to pH 7.0 at 100×10^{-6} M.

Before activation of DNA nanodevice, to exclude coated films onto counter and reference electrodes, electrodes were cut off and replaced with new ones combining with coated working electrode. To activate DNA nanodevice by releasing complementary sequence, 100 µL of DNA buffer was placed on the horizontal position of chip-electrode. Electroactivation was applied by specific potential for 30 s using a portable potentiostat (Palmsens 3, Palmsens) and then buffer was collected by pipette. The rinsing step was implemented once with equal volume of DNA buffer put on the chip-electrode for 2 min without any potential. In this way, electrical inputs were provided on the chip-electrodes changing the range from 0 to 0.7 V and from 0 to −0.7 V at 0.1 V intervals for each electrode using an amperometric detection/chronoamperometry technique in a PS trace 4.7 software (Palmsens).

Each of collected 100 uL DNA buffer containing complementary sequence was diluted with 250 µL of DNA buffer and put in a 96

DOI: 10.1002/smll.201601273

well plate with three repeats of 100 µL per well. 1 µL of 1×10^{-6} M DNA nanodevice was put in each well (10×10^{-9} M). When the released DNA complementally interacted with DNA nanodevice, fluorescence was detected using a plate reader (Synergy H1, BioTek) at an excitation wavelength of 485 nm and an emission wavelength of 520 nm in a temperature of 28 °C. Fluorescence was measured at 5 min intervals within a fixed period of 60 min.

As control experiment, a prepared chip-electrode was dipped in the 350 µL of DNA buffer to observe released DNA by diffusion effect. The chip-electrode was dipped four times for 5 min each, totally for 20 min.

To quantify activated DNA nanodevice, a binding curve was produced using 1, 3, 10, 30, 100, 300×10^{-9} M of cDNA with 10×10^{-9} M DNA nanodevice. Each concentration of cDNA was put in a 96 well plate by repeating three times 100 µL respectively. 1 µL of 1×10^{-6} M DNA nanodevice was added to each well and measured plate reader at 5 min intervals up to 45 min (Figure S1, Supporting Information). An equation was induced from this binding curve based on Langmuir model.

Supporting Information

Supporting Information is available from the Wiley Online Library or from the author.

Acknowledgements

This research was supported by the Bio & Medical Technology Development Program of the National Research Foundation of Korea (NRF) funded by the Korean Government (Grant 2012M3A9C6050104, 2013R1A1A1076126, 2014K2A7A1044460, 2016M3A9C6917405). Additionally, this research was also supported by a grant of the Korea Health Technology R&D Project through the Korea Health Industry Development Institute (KHIDI), funded by the Ministry of Health & Welfare, Republic of Korea (Grant HI14C-3266, HI15C-1653). This work was also carried out with the support of "Cooperative Research Program for Agriculture Science & Technology Development (Grant PJ00998601)" Rural Development Administration, Republic of Korea. This research was also supported by the Commercializations Promotion Agency for R&D Outcomes (COMPA) funded by the Ministry of Science, ICT and Future Planning (MSIP) (Grant 2016K000133). This research was also supported by EC-Korea agreement and ERC project ERC-2013-StG-336493-NATURE NANODEVICES.

[1] S. Modi, C. Nizak, S. Surana, S. Halder, Y. Krishnan, *Nat. Nanotechnol.* **2013**, *8*, 459.
[2] S. Bi, Y. Cui, Y. Dong, N. Zhang, *Biosens. Bioelectron.* **2014**, *53*, 207.
[3] M. You, L. Peng, N. Shao, L. Zhang, L. Qiu, C. Cui, W. Tan, *J. Am. Chem. Soc.* **2014**, *136*, 1256.
[4] D. Liu, S. Balasubramanian, *Angew. Chem. Int. Ed.* **2003**, *42*, 5734.
[5] J. Bath, A. J. Turberfield, *Nature* **2007**, *2*, 275.
[6] C. Zhao, Y. Song, J. Ren, X. Qu, *Biomaterials* **2009**, *30*, 1739.
[7] C.-H. Lu, B. Willner, I. Willner, *ACS Nano* **2013**, *7*, 8320.
[8] L. Song, V. H. B. Ho, C. Chen, Z. Yang, D. Liu, R. Chen, D. Zhou, *Adv. Healthcare Mater.* **2013**, *2*, 275.
[9] H. Zhang, M. Lai, A. Zuehlke, H. Peng, X.-F. Li, X. C. Le, *Angew. Chem. Int. Ed.* **2015**, *127*, 14534.
[10] E. D. Grosso, A.-M. Dallaire, A. Vallée-Bélisle, F. Ricci, *Nano Lett.* **2015**, *15*, 8407.
[11] J. Xu, Z. S. Wu, W. Shen, H. Xu, H. Li, L. Jia, *Biosens. Bioelectron.* **2015**, *73*, 19.
[12] J. Wu, F. Yu, Z. Zhang, Y. Chen, J. Du, A. Maruyama, *Nanoscale* **2016**, *8*, 464.
[13] S. Ranallo, A. Amodio, A. Idili, A. Porchetta, F. Ricci, *Chem. Sci.* **2016**, *7*, 66.
[14] G. Decher, *Science* **1997**, *277*, 1232.
[15] M. L. Macdonald, N. M. Rodriguez, N. J. Shah, P. T. Hammond, *Biomacromolecules* **2010**, *11*, 2053.
[16] B. B. Hsu, M.-H. Park, S. R. Hagerman, P. T. Hammond, *Proc. Natl. Acad. Sci.* **2014**, *111*, 12175.
[17] J. Cui, Y. Yan, G. K. Such, K. Liang, C. J. Ochs, A. Postma, F. Caruso, *Biomacromolecules* **2012**, *13*, 2225.
[18] Z. G. Estephan, Z. Qian, D. Lee, J. C. Crocker, S.-J. Park, *Nano Lett.* **2013**, *13*, 4449.
[19] A. P. R. Johnston, E. S. Read, F. Caruso, *Nano Lett.* **2005**, *5*, 953.
[20] J. Huang, Q. Shu, L. Wang, H. Wu, A. Y. Wang, H. Mao, *Biomaterials* **2015**, *39*, 105.
[21] B.-S. Kim, S. W. Park, P. T. Hammond, *ACS Nano* **2008**, *2*, 386.
[22] M. Macdonald, N. M. Rodriguez, R. Smith, P. T. Hammond, *J. Controlled Release* **2008**, *131*, 228.
[23] M. Choi, K.-G. Kim, J. Heo, H. Jeong, S. Y. Kim, J. Hong, *Sci. Rep.* **2015**, *5*, 17631.
[24] J. F. Quinn, F. Caruso, *Langmuir* **2004**, *20*, 20.
[25] D. M. Lynn, R. Langer, *J. Am. Chem. Soc.* **2000**, *122*, 10761.
[26] M. Zheng, A. Jagota, E. D. Semke, B. A. Diner, R. S. Mclean, S. R. Lustig, R. E. Richardson, N. G. Tassi, *Nat. Mater.* **2003**, *2*, 338.
[27] Z. Tang, H. Wu, J. R. Cort, G. W. Buchko, Y. Zhang, Y. Shao, I. A. Aksay, J. Liu, Y. Lin, *Small* **2010**, *6*, 1205.
[28] M. Wu, R. Kempaiah, P.-J. J. Huang, V. Maheshwari, J. Liu, *Langmuir* **2011**, *27*, 2731.
[29] J. Hong, N. J. Shah, A. C. Drake, P. C. DeMuth, J. B. Lee, J. Chen, P. T. Hammond, *ACS Nano* **2012**, *6*, 81.
[30] J. Watanabe, H. Shen, M. Akashi, *J. Mater. Sci.: Mater. Med.* **2009**, *20*, 759.
[31] D. J. O'Shannessy, M. Brigham-Burke, K. K. Soneson, P. Hensley, I. Brooks, *Anal. Biochem.* **1993**, *212*, 457.
[32] Y. Fei, Y. -S. Sun, Y. Li, K. Lau, H. Yu, H. A. Chokhawala, S. Huang, J. P. Landry, X. Chen, X. Zhu, *Mol. BioSyst.* **2011**, *7*, 3343.
[33] X. Luo, X. T. Cui, *Electrochem. Commun.* **2009**, *11*, 402.
[34] N. I. Kovtyukhova, P. J. Ollivier, B. R. Martin, T. E. Mallouk, S. A. Chizhik, E. V. Buzaneva, A. D. Gorchinskiy, *Chem. Mater.* **1999**, *11*, 771.
[35] B. Esteban Fernández de Ávila, H. M. Watkins, J. M. Pingarrón, K. W. Plaxco, G. Palleschi, F. Ricci, *Anal. Chem.* **2013**, *85*, 6593.

Received: April 13, 2016
Revised: June 20, 2016
Published online: